

Microstructure, electrical properties, and degradation behavior of praseodymium oxides-based zinc oxide varistors doped with Y_2O_3

CHOON-WOO NAHM, CHOON-HYUN PARK

Department of Electrical Engineering, Dongeui University, Pusan 614-714, Korea

E-mail: cwnahm@hyomin.dongueui.ac.kr

The microstructure, electrical properties, and degradation behavior of Pr-based zinc oxide varistors, which are composed of Zn-Pr-Co-Cr-Y oxides were investigated according to Y_2O_3 additive content in the range of 0.5–4.0 mol%. The majority of the added Y_2O_3 were segregated at the multiple ZnO grain junctions and grain boundaries. The average grain size was markedly decreased in the range of 27.3–8.6 μm with increasing Y_2O_3 additive content. Y_2O_3 acted as an inhibitor of grain growth. Additions of Y_2O_3 increased the varistor voltage in the range of 36.90–686.58 V/mm, increased the nonlinear exponent in the range of 3.75–87.42, decreased the leakage current in the range of 115.48–0.047 μA , increased the barrier height in the range of 1.06–2.16 eV, and decreased the donor concentration in the range of 1.87×10^{18} – $0.19 \times 10^{18} \text{ cm}^{-3}$. Y_2O_3 acted as an acceptor, as a result of the decrease of donor concentration. All Pr-based ZnO varistors doped with Y_2O_3 exhibited very predominant degradation characteristics, which show nearly symmetric I - V characteristics after the stress. In particular, since 4.0 mol% Y_2O_3 -added ZnO varistor has not only very excellent non-ohmicity, but also very stable degradation behavior, it is estimated to be sufficiently used to various application fields. © 2000 Kluwer Academic Publishers

1. Introduction

ZnO varistors are ceramic semiconductor devices manufactured by sintering ZnO powder with small additive amounts of other metal oxides, such as Bi_2O_3 , CoO, MnO, Sb_2O_3 , and Cr_2O_3 , etc. [1–3]. The sintering process gives rise to a microstructure, which consists of semiconducting n -type ZnO grains surrounded by insulating thin intergranular layers and resultantly makes potential barriers for electron inducing from trap states at the grain boundaries. ZnO varistors, therefore, contain a three-dimensional series-parallel junction network, called the microvaristors [2–4]. Their electrical characteristics exhibit a very steep nonlinear current-voltage (I - V) relationship similar to back-to-back Zener diode. In other word, they act as insulators below the varistor voltage, called the breakdown voltage, and conductors thereafter. Generally, they have slightly low nonlinearity than Zener diode, but much greater energy absorption capability than it [2, 3]. They are, therefore, widely used as surge absorption devices in electronic circuits and electrical power systems against dangerous overvoltage surges, such as lightning surges, switching surges, electrostatic discharges, and electromagnetic transients [5]. Since discovery of ZnO varistor, many workers have been investigated the conduction mechanism [4, 6–10], the microstructure [11–13], the role of additive constituents [14–17],

and the degradation phenomena [18–21]. Most of these studies, however, were restricted to the ZnO- Bi_2O_3 system containing varistor-forming oxide, such as Bi_2O_3 . The electrical characteristics of ZnO varistors which workers desire, are mainly high nonlinearity, low leakage current, and high stability. Many approaches have been attempted to improve these characteristics in Bi-based ZnO varistors.

Recently, several reports have been published for another type of ZnO varistors, which contains praseodymium oxide (Pr_6O_{11}) instead of Bi_2O_3 [22–24], but yet have not been surveyed in detail for various aspects. So far, the compositions of most studied Pr-based ZnO varistors were almost limited to ternary system, such as ZnO- Pr_6O_{11} -CoO.

The purpose of this paper is to investigate the effects of Y_2O_3 additive content on the microstructure, current-voltage (I - V) characteristics, capacitance-voltage (C - V) characteristics, and degradation behavior of Praseodymium oxides-based ZnO varistors, which are consisted of compositions, such as ZnO, Pr_6O_{11} , CoO, Cr_2O_3 , and Y_2O_3 .

2. Experimental procedure

2.1. Sample preparation

Reagent-grade raw materials were prepared for ZnO varistors with composition expression, such as

(94.0- x) mol% ZnO + 0.5 mol% Pr₆O₁₁ + 5.0 mol% CoO + 0.5 mol% Cr₂O₃ + x mol% Y₂O₃ ($x = 0.5, 1.0, 2.0, 4.0$). Raw materials were mixed by ball milling with zirconia balls and acetone in a polypropylene bottle for 24 h. The mixture was dried at 120 °C for 12 h and calcined in air at 750 °C for 2 h. The calcined mixture was pulverized using agate mortar/pestle and after 2 wt% PVA binder addition, granulated by sieving 100-mesh screen to produce the starting powder. The powder was pressed into discs of 10 mm diameter and 2 mm thickness at a pressure of 800 kg/cm². The discs were placed in the starting powder using an alumina crucible, sintered in air at 1350 °C for 1 h, and furnace-cooled to room temperature. The heating and cooling rates were 4 °C/min and 2.5 °C/min, respectively. The sintered samples were lapped and polished to 1.0 mm thickness. The silver paste was coated to both faces of samples and the silver electrode was formed by heating at 600 °C for 10 min.

2.2. I - V characteristics measurement

The I - V characteristics of the varistors were measured using an I - V source/measure unit (Keithley 237) in the temperature range of 0 °C to 150 °C. The varistor voltage ($V_{1\text{ mA}}$) was measured at 1.0 mA/cm² and the leakage current (I_l) was measured at 80% of varistor voltage. In addition, the nonlinear exponent (α) is defined by the empirical law, $J = K \cdot E^\alpha$, where J is the current density, E is the applied electric field, and K is constant. α was determined in the current density range of 1.0 mA/cm² to 10 mA/cm², according to the following expression [1]:

$$\alpha = \frac{1}{(\log E_2 - \log E_1)} \quad (1)$$

where E_2 and E_1 are the electric field corresponding to 10 mA/cm² and 1.0 mA/cm², respectively.

2.3. C - V characteristics measurement

The C - V characteristics of varistors were measured at room temperature using an impedance analyzer (HP4194A Hewlett-Packard, Co.) at 1 kHz. The donor concentration (N_d) and the barrier height (ϕ_b) were determined from the slope and intercept of straight line, respectively, according to the following expression [25]:

$$\left(\frac{1}{C_b} - \frac{1}{2C_{bo}}\right)^2 = \frac{2}{q\varepsilon N_d}(\phi_b + V_g) \quad (2)$$

where C_b is the capacitance per unit area of a grain boundary, C_{bo} is the value of C_b when $V_g = 0$, V_g is the applied voltage per grain boundary, q is the electronic charge, ε is the permittivity of ZnO ($\varepsilon = 8.5\varepsilon_0$).

The density of interface states (N_t) at the grain boundary can be estimated using the value of the donor concentration and barrier height, according to the following expression [25]:

$$N_t = \sqrt{\frac{2\varepsilon N_d \phi_b}{q}} \quad (3)$$

Once the donor concentration and barrier height are known, the depletion layer width (t) of either side at the grain boundaries can be obtained from the following expression [26]:

$$t = \sqrt{\frac{2\varepsilon\phi_b}{qN_d}} \quad (4)$$

2.4. Degradation phenomena measurement

DC degradation tests were independently performed under the two stress conditions, such as 0.80 $V_{1\text{ mA}}/100$ °C/12 h and 0.80 $V_{1\text{ mA}}/100$ °C/12 h + 0.85 $V_{1\text{ mA}}/120$ °C/12 h. At the same time, the leakage current during the stress time, was monitored at interval of 1 min by an I - V source/measure unit (Keithley 237). After the respective stress, the I - V characteristics were measured at the room temperature.

2.5. Microstructure examination

To investigate the surface morphology, the either surface of samples that the electrical measurement has been finished was lapped and ground with SiC paper and polished with 0.3 μm -Al₂O₃ powder to a mirrorlike surface. The polished samples were thermally etched at 1150 °C for 30 min. The surface of samples was metallized with a thin coating of Au to reduce charging effects and to improve the resolution of the image. The surface microstructure was examined by scanning electron microscopy (SEM, Model S2400, Hitachi, Japan). The average grain size (d) was determined by the lineal intercept method [27], as described below.

$$d = 1.56 \frac{L}{MN} \quad (5)$$

where L is the random line length on the micrograph, M is the magnification of the micrograph, and N is the number of the grain boundaries intercepted by lines. The compositional analysis of the selected areas was determined by an attached energy dispersion X-ray analysis (EDAX) system. The crystalline phases were identified by powder X-ray diffraction (XRD, Model D/max 2100, Rigaku, Japan).

3. Results and discussion

Fig. 1 shows the SEM micrographs of samples doped with Y₂O₃. As can be seen in this figure, two phases are only presented in the ceramics, that is, ZnO grain and an intergranular phase consisted mainly of Y₂O₃. These phases were revealed by XRD pattern shown in Fig. 2 and EDAX pattern shown in Fig. 3. The majority of the added Y₂O₃ were much more segregated at the multiple ZnO grain junctions than between two ZnO grains, and Y₂O₃ was not nearly solved in ZnO grains. With increasing Y₂O₃ additive content, the Y-rich phase was more distributed at the multiple ZnO grain junctions and the Y-rich phase between two ZnO grains was more discontinuously distributed. The grain size of these samples was relatively uniform without generating abnormal grain growth. The average grain size

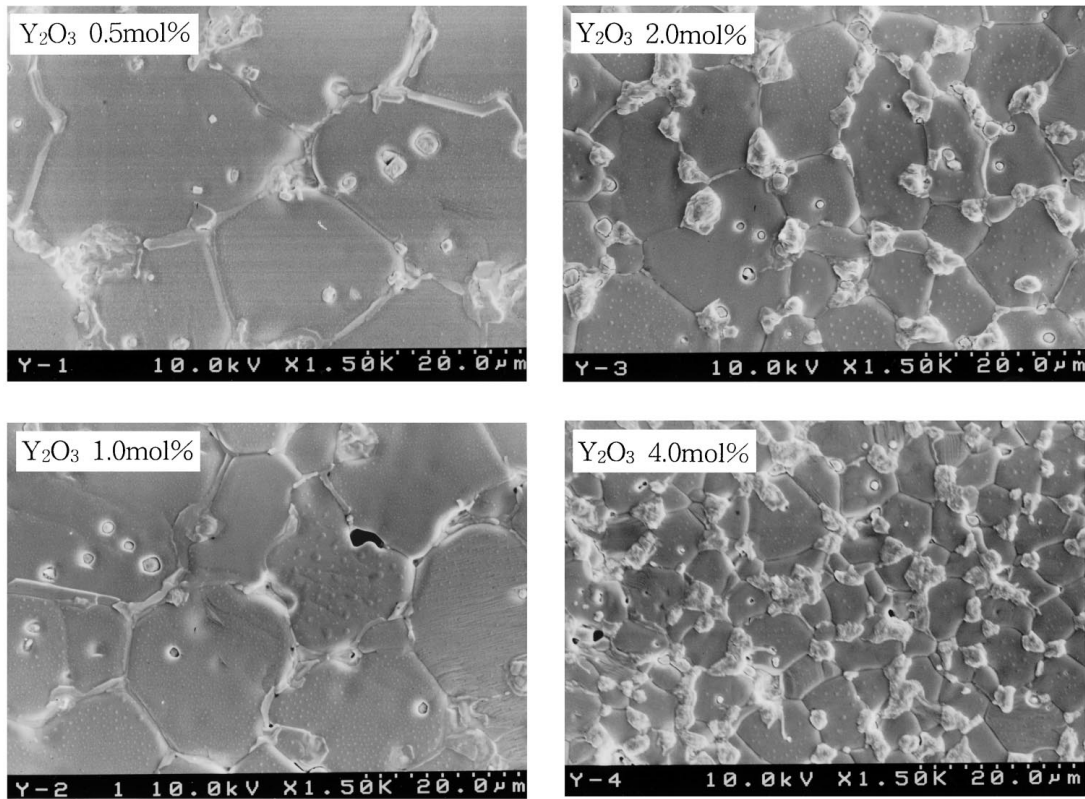


Figure 1 SEM micrographs of Pr-based ZnO varistor samples doped with Y_2O_3 .

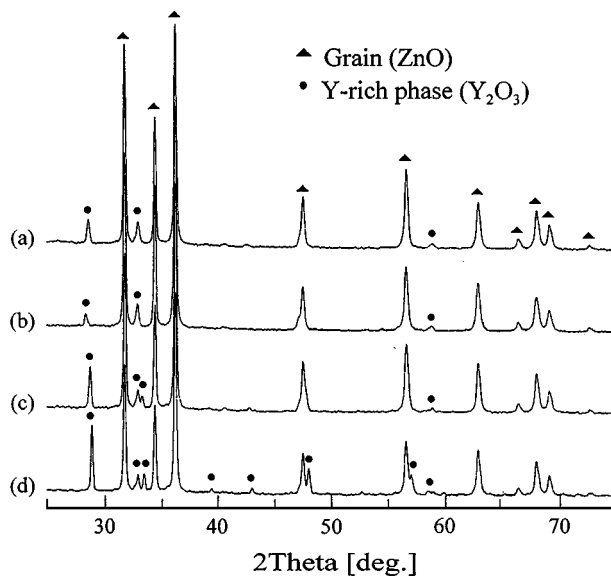


Figure 2 XRD patterns of Pr-based ZnO varistor samples doped with Y_2O_3 : (a) 0.5 mol%, (b) 1.0 mol%, (c) 2.0 mol%, and (d) 4.0 mol%.

was markedly decreased in the range of 27.3–8.6 μm as the Y_2O_3 additive content is increased. Consequently, Y_2O_3 acted as an inhibitor of grain growth.

The current-voltage (I - V) characteristics of Pr-based ZnO varistors doped with Y_2O_3 are shown in Fig. 4. It intuitively can be seen that the I - V characteristics are saliently improved as the Y_2O_3 additive content is increased. Table I shows the I - V characteristic parameters determined from the I - V characteristics. As the Y_2O_3 additive content is increased, the varistor voltage ($V_{1\text{mA}}$) and the breakdown voltage per grain boundary abruptly increased in the range of 36.90–686.58 V/mm and 1.29–5.90 V/gb, respectively. The breakdown volt-

TABLE I I - V characteristic parameters of Pr-based ZnO varistors doped with Y_2O_3

Y_2O_3 content (mol%)	$V_{1\text{mA}}$ (V/mm)	v_{gb} (V/gb)	E_a (eV)	I_t (μA)	α
0.5	36.90	1.29	0.33	115.48	3.75
1.0	77.33	2.11	0.35	55.03	9.29
2.0	251.55	3.72	0.57	1.95	43.81
4.0	686.58	5.90	0.67	0.047	87.42

age per grain boundary (v_{gb}) was determined as the following expression:

$$v_{\text{gb}} = \frac{V_{1\text{mA}}}{n} = \frac{d}{D} \cdot V_{1\text{mA}} \quad (6)$$

where n is the number of grain boundaries arranged as the series between both electrodes, d is the average grain size, and D is the sample thickness.

The activation energy (E_a), called the average energy that electrons can over the Schottky barrier, is evaluated from the investigation of the temperature dependence of I - V characteristics, at low voltage, i.e., at the prebreakdown region, as described the following expression:

$$J = A^* T^2 \exp(-E_a/kT) \cdot \exp(\beta_s E^{1/2}/kT) \\ = A^* T^2 \exp(-E_a/kT) |_{E=0} \quad (7)$$

where A^* is the Richardson constant, T is the absolute temperature, k is the Boltzmann constant, β_s is the Schottky coefficient, and E is the applied voltage.

Fig. 5 represents the Arrhenius plot $\ln J$ versus $1/T$ drawn in order to determine the activation energy, according to the expression (7). From the slope of Fig. 5, the activation energy was increased in the range of 0.33–0.67 eV with increasing Y_2O_3 additive content.

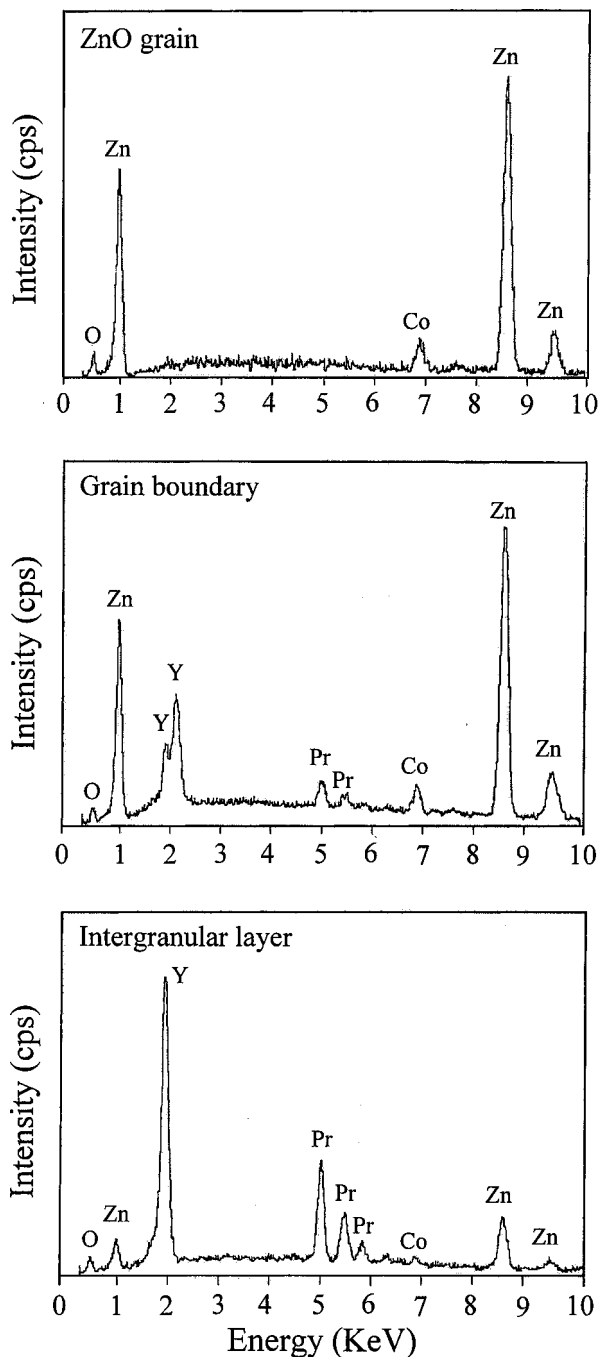


Figure 3 EDAX analysis of Pr-based ZnO varistor sample containing 4.0 mol% Y_2O_3 .

Meanwhile, the leakage current was decreased in the range of $115.48\text{--}0.047\ \mu\text{A}$ as the Y_2O_3 additive content is increased. It is believed that the decrease of leakage current is attributed to the increase of activation energy. In particular, 4.0 mol% Y_2O_3 -added varistor exhibited the excellent insulating properties at low voltages. Since the leakage current is directly related to the degradation and the reliability, which will be mentioned afterward, it is particularly important to realize that the leakage current should be as low as possible to the various applications.

One of the important performance figures of ZnO varistor is the nonlinear exponent, which is the essential property of the varistor. When Y_2O_3 was added less than 2.0 mol%, the nonlinear exponent was very poor, but more than 2.0 mol%, was markedly enhanced and at the level of 4.0 mol%, was 87.42.

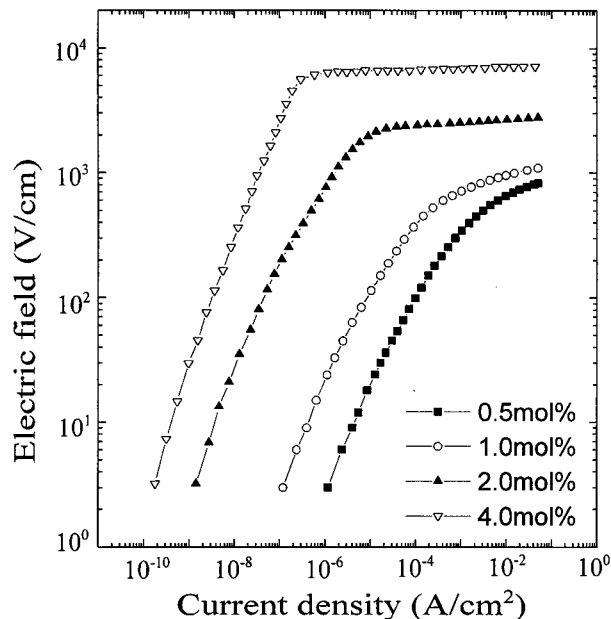


Figure 4 I-V characteristics of Pr-based ZnO varistors doped with Y_2O_3 .

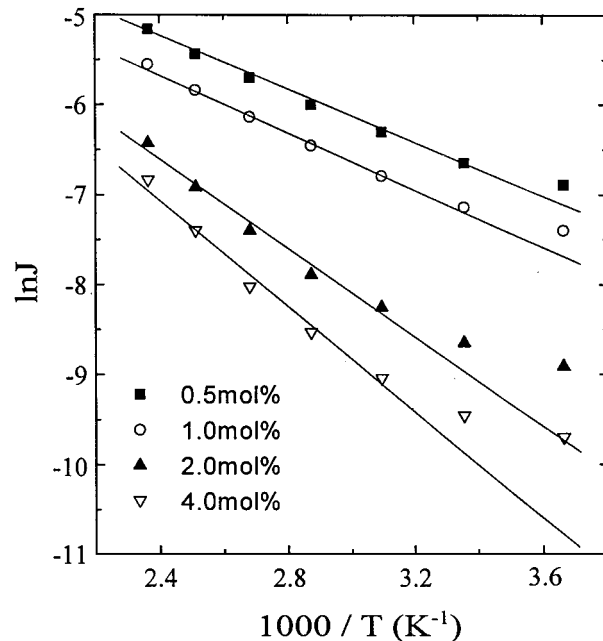


Figure 5 Arrhenius plot of $\ln J$ of Pr-based ZnO varistors doped with Y_2O_3 .

The capacitance-voltage (C - V) characteristics of Pr-based ZnO varistors doped with Y_2O_3 are shown in Fig. 6. Table II shows the C - V characteristic parameters determined from C - V characteristics. As the Y_2O_3 additive content is increased, the donor concentration was largely decreased in the range of 1.87×10^{18} – $0.19 \times 10^{18}\ \text{cm}^{-3}$. Generally, when a trivalent ion is soluble in ZnO grains, a trivalent ion will act as a donor. Based on the decrease of donor concentration with increasing Y_2O_3 additive content, it is thought that Y_2O_3 addition to ZnO is not likely to involve accommodation of Y ions on host lattice sites. In this case, a trivalent Y^{+3} ion will not substitute a divalent Zn^{+2} ion allowing an electron to move to the conduction band. If so, what is the cause for the decrease of donor concentration? It is thought that this is probably related to the partial pressure of oxygen. Anyway, Y_2O_3 in

TABLE II *C-V* characteristic parameters of Pr-based ZnO varistors doped with Y_2O_3

Y_2O_3 content (mol%)	N_d ($\times 10^{18} \text{cm}^{-3}$)	N_t ($\times 10^{12} \text{cm}^{-2}$)	ϕ_b (eV)	t (nm)
0.5	1.87	4.32	1.06	35.76
1.0	1.43	4.58	1.56	48.01
2.0	0.39	2.12	1.21	86.54
4.0	0.19	1.98	2.16	149.74

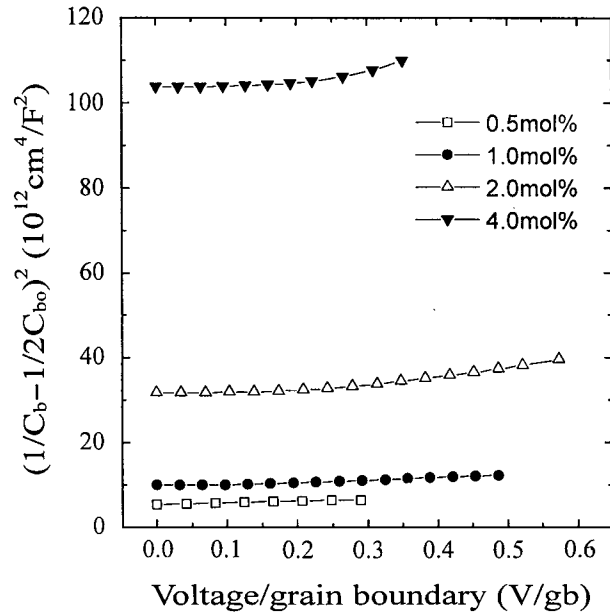


Figure 6 Modified *C-V* characteristics of Pr-based ZnO varistors doped with Y_2O_3 .

ZnO grain acts as an acceptor, the density of interface states exhibited a tendency decreasing in the range of $4.32 \times 10^{12} - 1.98 \times 10^{12} \text{cm}^{-2}$.

While the barrier height is connected with donor the concentration and density of interface states. The barrier height is estimated by the variation rate in the density of interface states and donor concentration as represented expression (3). Generally, the barrier height is increased with increasing density of interface states and decreasing donor concentration. If the variation rate of donor concentration is much larger than that of density of interface states with an additive content, the barrier height is much more strongly affected to donor concentration than density of interface states. According to this reason, it would be understood that the barrier height is increased or decreased with increasing Y_2O_3 additive content. The increase of depletion layer width with increasing Y_2O_3 additive content is attributed to the decreased of donor concentration.

Fig. 7 shows the *I-V* characteristics of Pr-based ZnO varistors doped with Y_2O_3 before and after the stress. It intuitively can be seen that after the stress, the variation of *I-V* curve is very small regardless of the bias directions and the stress conditions. It is well known facts that the nonlinear *I-V* characteristics are mainly governed by Schottky barrier at the grain boundaries. Therefore, the variation in the *I-V* curve is directly related to the deformation of Schottky barrier. Since the applied DC voltage is mostly dropped to the reverse-biased

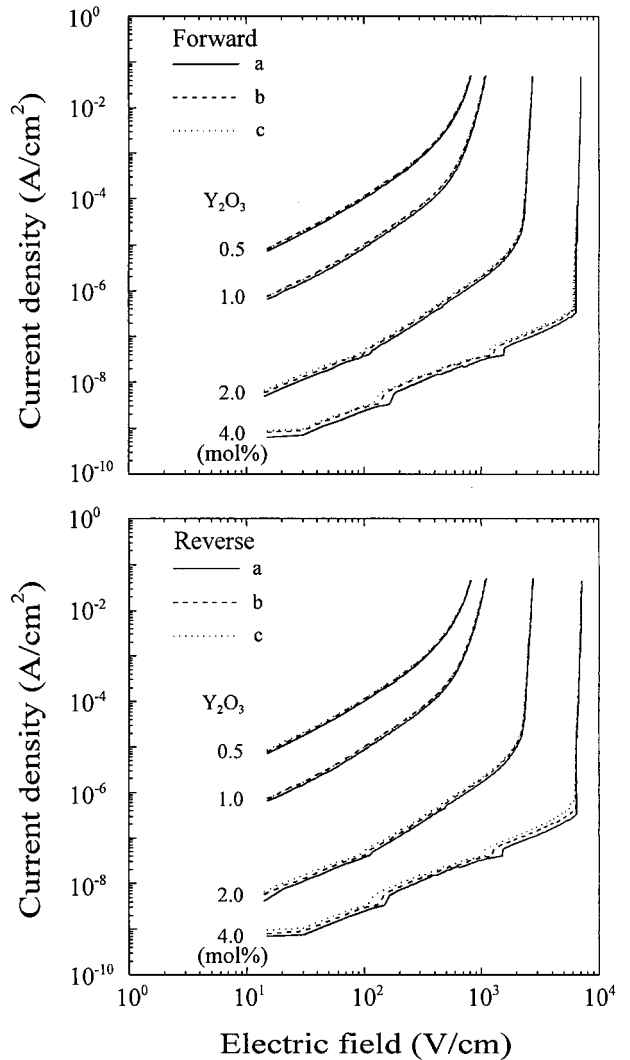


Figure 7 *I-V* characteristics of Pr-based ZnO varistors doped with Y_2O_3 before and after the stress: (a) before stress, (b) $0.80 V_{1\text{mA}}/100^\circ\text{C}/12\text{h}$, and (c) $0.80 V_{1\text{mA}}/100^\circ\text{C}/12\text{h} + 0.85 V_{1\text{mA}}/120^\circ\text{C}/12\text{h}$.

Schottky barrier, the variation rate of a voltage for the *I-V* curve in the reverse direction is larger than that the forward direction corresponding to the same current.

For 2.0 mol% Y_2O_3 -added varistor, after the second stress, in the reverse direction, the variation rate of varistor voltage was less than 1% and that of nonlinear exponent was less than 5%. For 4.0 mol% Y_2O_3 -added varistor, after the second stress, in the reverse direction, the variation rate of varistor voltage was about 0.5% and that of nonlinear exponent was about 5%. The Pr-based ZnO varistors doped with Y_2O_3 show nearly symmetric *I-V* characteristics, which were slightly degraded in the reverse direction. Therefore, it can be seen that Pr-based ZnO varistors doped with Y_2O_3 above 2.0 mol% show good and stable *I-V* characteristics.

The time dependence of the leakage current during the stress is shown in Fig. 8. It should be noted that the leakage current represents a nearly constant value regardless of the Y_2O_3 additive content. In other words, the positive creep phenomena of leakage current were not observed in the all samples. The degradation of ZnO varistors is associated with the lowering of the potential barrier at the grain boundaries, which is related to the annihilation of interface defect states when

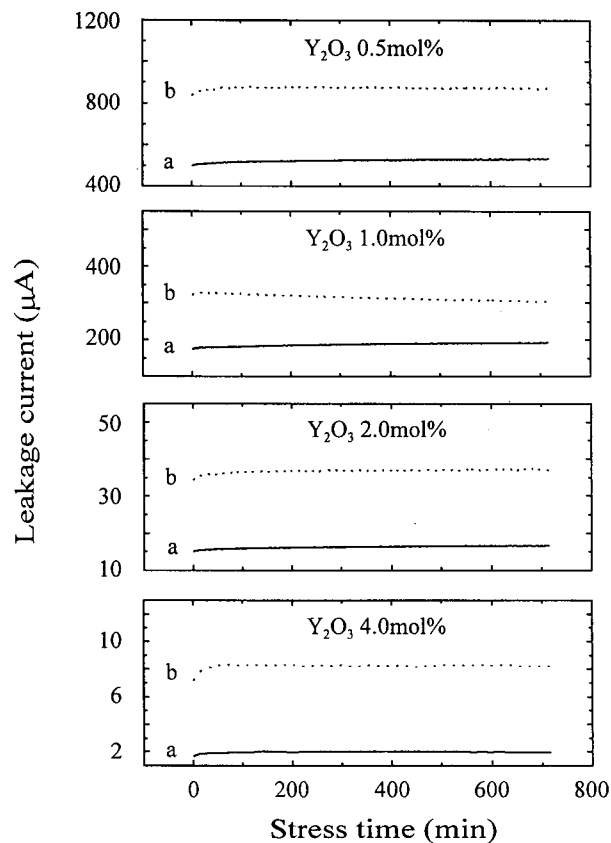


Figure 8 Time dependence of leakage current during the stress: (a) 0.80 $V_{1mA}/100\text{ }^{\circ}\text{C}/12\text{ h}$ and (b) 0.80 $V_{1mA}/100\text{ }^{\circ}\text{C}/12\text{ h} + 0.85\text{ }V_{1mA}/120\text{ }^{\circ}\text{C}/12\text{ h}$.

stressed continuously by an electric field. So far, among mechanisms proposed to explain the degradation, the most probable mechanism is accepted to be ion migration mechanism proposed by Gupta and Carlson [18]. According to this, when ZnO varistor is stressed continuously by an electric field, the positively charged zinc interstitial (Zn_i) formed and frozen in the depletion layer during cooling from sintering temperature, migrates toward the negatively charged grain boundary interface, and it recombines with zinc vacancy (V_{Zn}) positioned in there. As a result, the recombination of these species leads to the degradation of ZnO varistor. In the light of these facts, It is guessed that the reason why Pr-based ZnO varistors doped with Y_2O_3 exhibit predominant degradation characteristics, is to be because the added Y_2O_3 spatially restricts the migration of zinc interstitial (Zn_i) within depletion layer.

4. Conclusions

1. The majority of Y_2O_3 added to composition formulation of Pr-based ZnO varistors was much more segregated at the multiple ZnO grain junctions than between two ZnO grains. The phases, which present in the ceramics of Pr-based ZnO varistors doped with Y_2O_3 were only ZnO grain and intergranular phase consisted mainly of Y_2O_3 . The average grain size was markedly decreased in the range of 27.3–8.6 μm as the Y_2O_3 additive content is increased. Y_2O_3 acted as an inhibitor of grain growth.

2. Additions of Y_2O_3 to a composition formulation of Pr-based ZnO varistors increased the varistor voltage

and nonlinear exponent, and decreased the leakage current. What is remarkable, 4.0 mol% Y_2O_3 -added ZnO varistor marked the excellent non-ohmicity, which the nonlinear exponent reaches 87.42 and the leakage current reaches 0.047 μA .

3. Although the density of interface states is decreased with increasing Y_2O_3 additive content, the barrier height exhibited the increasing tendency due to the abrupt decrease of donor concentration. This coincided with the increasing tendency of the activation energy in I - V characteristics. Y_2O_3 acted as an acceptor, as a result of the decrease of donor concentration.

4. All Pr-based ZnO varistors doped with Y_2O_3 exhibited very predominant degradation characteristics, which show nearly symmetric I - V characteristics after the stress. What is remarkable, the leakage current with time during the applied stress, was observed to be constant in all samples. In particular, since 4.0 mol% Y_2O_3 -added ZnO varistor has not only very excellent non-ohmicity, but also very stable degradation behavior, it is estimated to be sufficiently used to various application fields.

References

1. M. MATSUOKA, *Jpn. J. Appl. Phys.* **10** (1971) 736.
2. L. M. LEVINSON and H. R. PHILIPP, *Am. Ceram. Soc. Bull.* **65** (1986) 639.
3. T. K. GUPTA, *J. Am. Ceram. Soc.* **73** (1990) 1817.
4. L. K. J. VANADAMME and J. C. BRUGMAN, *J. Appl. Phys.* **51** (1980) 4240.
5. S.-N. BAI and T.-Y. TSENG, *Jpn. J. Appl. Phys.* **31** (1992) 81.
6. L. M. LEVINSON and H. R. PHILIPP, *J. Appl. Phys.* **46** (1975) 1332.
7. M. FIX and J. SOLN, *Appl. Phys. Lett.* **26** (1075) 519.
8. P. R. EMTAGE, *J. Appl. Phys.* **48** (1977) 4372.
9. K. EDA, *ibid.* **49** (1978) 2964.
10. G. D. MAHAN, L. M. LEVINSON and H. R. PHILIPP, *ibid.* **50** (1979) 2799.
11. J. WONG, *ibid.* **46** (1975) 1653.
12. M. INADA, *Jpn. J. Appl. Phys.* **17** (1978) 1.
13. *Idem.*, *ibid.* **17** (1978) 673.
14. C.-Y. SHEN, Y.-C. CHEN and L. WU, *ibid.* **32** (1993) 2043.
15. J. FAN and R. FREER, *J. Appl. Phys.* **77** (1995) 4795.
16. T. R. KUTTY and S. EZHILVALAVAN, *Jpn. J. Appl. Phys.* **34** (1995) 6125.
17. S. A. PIANARO, E. C. PEREIRA, L. O. S. BULHOES, E. LONGE and J. A. VARELA, *J. Mat. Sci.* **30** (1995) 133.
18. T. K. GUPTA and W. G. CARLSON, *ibid.* **20** (1985) 3487.
19. Y.-S. LEE and T.-Y. TSENG, *J. Am. Ceram. Soc.* **75** (1992) 1636.
20. J. FAN and R. FREER, *J. Mat. Sci.* **28** (1993) 1391.
21. C.-S. CHEN, C.-T. KUO and I.-N. LIN, *J. Mat. Res.* **13** (1998) 1560.
22. A. B. ALLES and V. L. BURDICK, *J. Appl. Phys.* **70** (1991) 6883.
23. A. B. ALLES, R. PUSKAS, G. CALLAHAN and V. L. BURDICK, *J. Am. Ceram. Soc.* **76** (1993) 2098.
24. Y.-S. LEE, K.-S. LIAO and T.-Y. TSENG, *ibid.* **79** (1996) 2379.
25. M. MUKAE, K. TSUDA and I. NAGASAWA, *J. Appl. Phys.* **50** (1979) 4475.
26. S. M. SZE, in "Physics of Semiconductor Devices" (John Wiley and Sons, New York, 1981) p. 402.
27. J. C. WURST and J. A. NELSON, *J. Am. Ceram. Soc.* **97-12** (1972) 109.

Received 22 April

and accepted 13 December 1999